International Journal of Bifurcation and Chaos, Vol. 4, No. 3 (1994) 489–519

CHUA'S CIRCUIT: RIGOROUS RESULTS AND FUTURE PROBLEMS

LEONID P. SHIL'NIKOV
Department of Differential Equations,
Research Institute for Applied Mathematics & Cybernetics,
10 Ul'janov St., Nizhny Novgorod 603005, Russia

Received November 25, 1993; Revised December 15, 1993

Mathematical problems arising from the study of complex dynamics in Chua's circuit are discussed. An explanation of the extreme complexity of the structure of attractors of Chua's circuit is given. This explanation is based upon recent results on systems with homoclinic tangencies. A number of new dynamical phenomena is predicted for those generalizations of Chua's circuits which are described by multidimensional systems of ordinary differential equations.

1. Introduction

One of the most remarkable achievements of science in the twentieth century is the discovery of dynamical chaos. Using this paradigm, many problems in modern science and engineering which can be modelled via the language of nonlinear dynamics have obtained an adequate mathematical description. However, the explanation of a number of phenomena of dynamical chaos has required the creation of new mathematical techniques. The reason for this is that the classical theory of nonlinear oscillations developed by van der Pol, Andronov, Pontryagin, Krylov, Bogolyubov *et al.*, was based on Poincaré's theory of periodic orbits and Lyapunov's stability theory, i.e., on methods for studying mainly *quasi-linear* systems.

Problems associated with systems involving high energies, powers, velocities, etc., must be modelled by multidimensional and *strongly nonlinear* differential equations (ordinary, partial, etc.). The study of such systems has generated numerous new concepts and terminologies: hyperbolic sets, symbolic dynamics, homoclinic and heteroclinic orbits, global bifurcations, entropy (topological and metric), Lyapunov exponents, fractal dimensions, etc. We note the possibility of describing dynamical chaos via statistical tools as well; e.g., correlation function, power spectrum and so on. They are widely used in numerical simulations and in experiments.

Here, we should note the concrete phenomena and models that have played important roles in establishing dynamical chaos in different fields of knowledge. They are the *Lorenz model* in hydrodynamics and in the theory of lasers, the *Belousov–Zhabotinsky reaction* in chemistry and biophysics, the *Chua circuit* in radiophysics and nonlinear electronics, etc.

Chua's circuit has become very popular since the middle of the 80's (see Chua [1992], Nolta [1993], Madan [1993a, 1993b], Chua & Hasler [1993]). Being, in its physical nature, a rather simple electronic oscillator (in the simplest case it consists of only four linear elements and one nonlinear element, as shown in Fig. 1), Chua's circuit is a very suitable subject for study by means of both laboratory experiments and computer simulations. This is because Chua's circuit admits an adequate modelling via the language of differential equations. In the simplest case Chua's equations are written in the

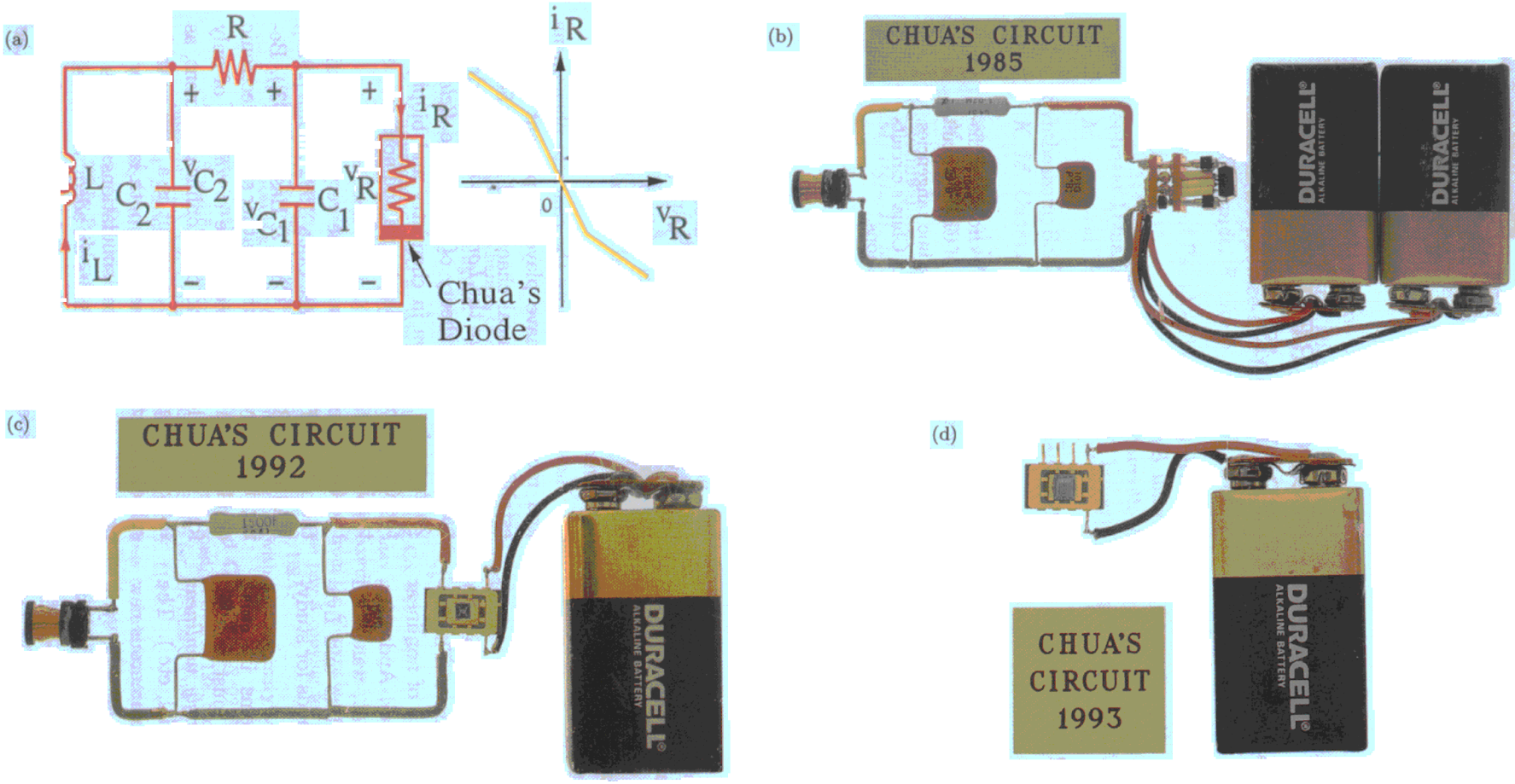

Fig. 1. Chua's Circuit and its evolution. (a) Original circuit designed by Chua in 1983 consists of, from left to right, a linear inductor L (with *current* i_L), a linear capacitor C_2 (with *voltage* v_{C_2}), a linear resistor R, a linear capacitor C_1 (with *voltage* v_{C_1}), and a nonlinear resistor (Chua's diode) having a piecewise-linear voltage-versus-current characteristic. (b) Simplest physical implementation of Chua's circuit [Zhong & Ayrom, 1985] using standard electronic components in one-to-one correspondence to the ideal two-terminal circuit elements depicted in (a), except for the rightmost Chua's diode, which does not exist as a standard component, but which is synthesized in a subassembly made of a dual op amp (operational amplifier) package connected to 6 external linear resistors. The op amp package (AD712, TL082, or equivalent) is powered by two 9-volt batteries. (c) Same as in (b) except that the Chua's diode subassembly is replaced by a single IC chip (integrated circuit) [Cruz & Chua, 1992]. The IC chip inside the 8-pin DIP package measures 1.3 mm × 1.3 mm and is powered by *one* 9-volt battery. (d) The *entire* Chua's circuit realized in (b) using *discrete* electronic components is shown here being implemented in a single *monolithic* IC chip [Cruz & Chua, 1993]. The chip inside the 8-pin DIP package (1 cm × 2 cm external dimension) is fabricated using the standard 2-micron CMOS technology and occupies a silicon area of 2.5 mm × 2.8 mm. The Chua's Circuit IC Chip is powered by a single 9-volt battery and dissipates 0.001 Watts of electrical power. Using the latest 0.5 micron technology, a locally-connected array of 20,000 identical Chua's circuits can be fabricated in a single IC chip the size of a finger nail. The parameters of this monolithic VLSI chip of *Chua's circuit array* are programmable via external pins and is therefore an ideal vehicle for studying complex spatio-temporal phenomena. (*Courtesy of L. O. Chua*)

following dimensionless form

$$\boxed{\begin{aligned}\dot{x} &= \alpha(y - x - h(x))\\ \dot{y} &= x - y + z\\ \dot{z} &= -\beta y\end{aligned}} \tag{1}$$

where α and β are dimensionless parameters. The nonlinear function $h(x)$ has the form[1]

$$h(x) = m_1 x + \frac{1}{2}(m_0 - m_1)\{|x+1| - |x-1|\}\,,$$

where m_0 and m_1 denote the slope of the normalized piecewise-linear function.

The main reasons why Chua's circuit is a subject of not only engineering interest is the following:

1. Chua's circuit exhibits a number of different scenarios in the appearance of chaos; namely, transition to chaos through the period-doubling cascade, through the breakdown of an invariant torus, etc. All of these bifurcation phenomena makes the study of Chua's circuits a rather universal problem.
2. Chua's circuit exhibits a chaotic attractor called the "double scroll Chua's attractor" [Madan, 1993a]. It appears at the conjunction of a pair of nonsymmetric spiral attractors. Three equilibrium states of a saddle-focus type are visible in this attractor, which indicates that the double scroll Chua's attractor is *multistructural*, which distinguishes it from other known attractors of three-dimensional systems.
3. Equations (1) are rather close to the equations of a three-dimensional normal form (in the sense that the respective phase portraits of strange attractors are close) for bifurcations of an equilibrium state with three zero characteristic exponents (for the case with additional symmetry [Arneodo *et al.*, 1984]), and that for a periodic orbit with three multipliers equal to -1.
4. In their mathematical nature, the attractors which occur in Chua's circuits are essentially more complicated objects than they had seemed before. This conclusion is based on new subtle results on systems with homoclinic tangencies and homoclinic loops of a saddle-focus [Ovsyannikov & Shil'nikov, 1987; 1993; Gonchenko *et al.*, 1992; 1993a; 1993c; 1994].

The recent generalization obtained by adding a linear resistor R_0 to Chua's circuit, as shown in Fig. 2, is described by the following equations:

$$\begin{aligned}\frac{dv_1}{dt} &= \frac{1}{C_1}[G(v_2 - v_1) - f(v_1)]\,,\\ \frac{dv_2}{dt} &= \frac{1}{C_2}[G(v_1 - v_2) + i_3]\,,\\ \frac{di_3}{dt} &= -\frac{1}{L}(v_2 + R_0 i_3)\,,\end{aligned} \tag{2}$$

where

$$G = \frac{1}{R}$$

and

$$f(v_1) = G_b v_1 + \frac{1}{2}(G_a - G_b)\{|v_1 + E| - |v_1 - E|\}\,.$$

Here, the v–i characteristic f is odd-symmetric, consisting of three linear components, where the two slopes G_a and G_b may assume any sign and value.

Equation (2) is called a *global unfolding* of Chua's circuit [Chua, 1993]. In dimensionless form it is written as

$$\begin{aligned}\dot{x} &= k\alpha(y - x - h(x))\,,\\ \dot{y} &= k(x - y + z)\,,\\ \dot{z} &= k(-\beta y - \gamma z)\,,\end{aligned} \tag{3}$$

where h is the same as above and k is defined as follows:

$$k = \begin{cases} 1 & \text{if } RC_2 > 0\,,\\ -1 & \text{if } RC_2 < 0\,.\end{cases}$$

Let us denote the set of characteristic exponents of the equilibrium state O in the origin as $\lambda = (\lambda_1, \lambda_2, \lambda_3)$, and the set of characteristic exponents corresponding to $x > 1$ (or, what is the same, to $x < 1$) as $\nu = (\nu_1, \nu_2, \nu_3)$. It is well known that two Chua's circuits are equivalent if they have equal sets λ and ν. Therefore, it is natural to choose these sets as control parameters. Unfortunately, it cannot be done for the original Chua's circuit [Eq. (1)] since, in this case, a constraint exists among λ and ν, but the global unfolding (3) of Chua's circuit is free of this defect. Moreover, all of the 12-parameter

[1]From a *nonlinear circuit* perspective the nonlinear function $h(x)$ in Chua's equations can be *any* single-valued function of x because Chua has pioneered techniques for synthesizing such nonlinearities using *standard* electronic components as building blocks [Chua, 1969; Chua *et al.*, 1987]. For example, $h(x)$ is an odd-symmetric polynomial in Khibnik *et al.*, [1993], a nonsymmetric piecewise-linear function in Perez-Munuzuri *et al.* [1993], Mayer-Kress *et al.* [1993], a discontinuous function in Mahla & Badan-Palhares [1993], etc.

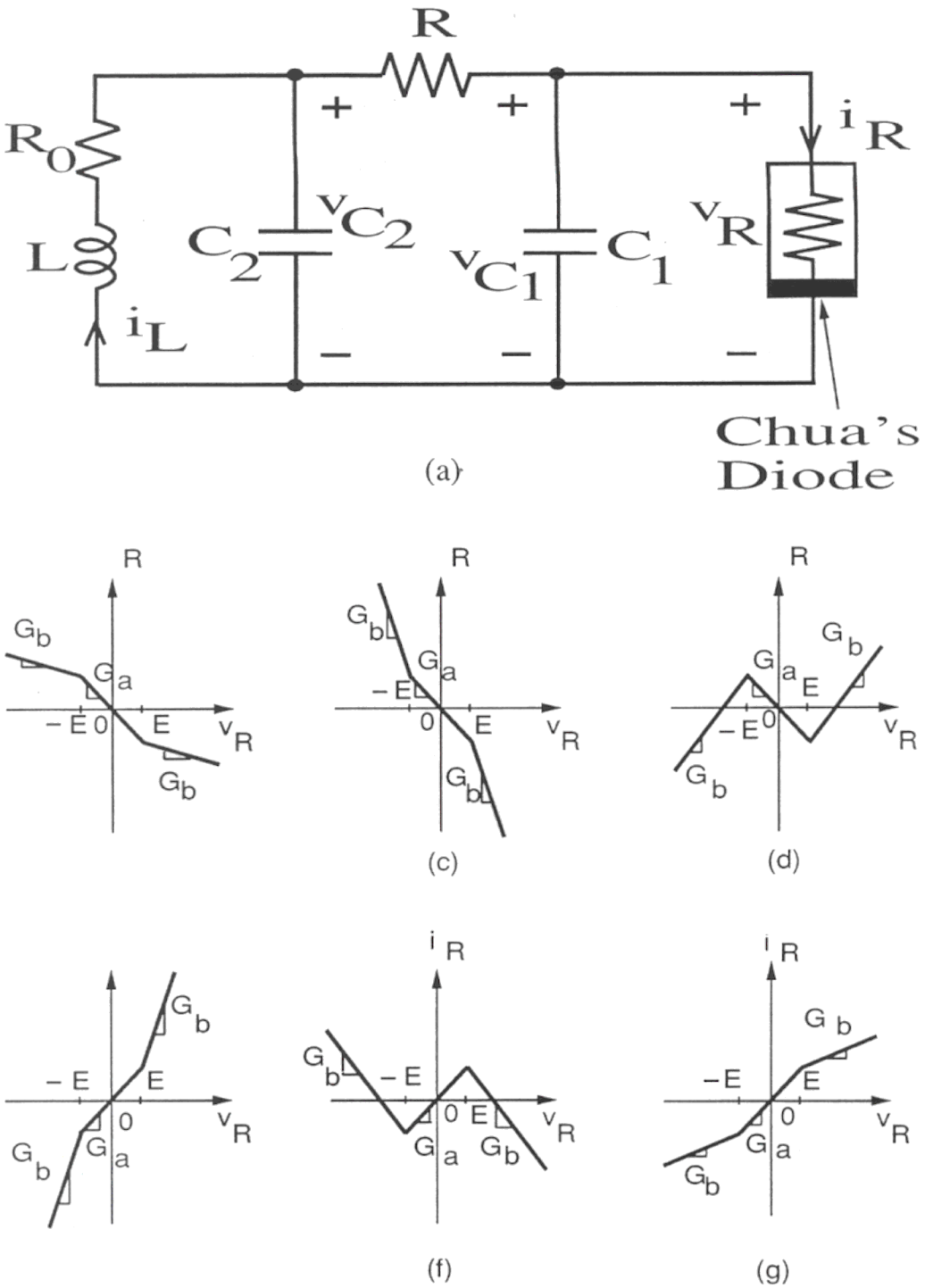

Fig. 2. (a) The unfolded Chua's circuit is obtained by inserting a linear resistor R_0 in series with the inductor L in the original Chua's circuit. In general, Chua's diode may be characterized by an *arbitrary* (not necessarily continuous, piecewise-linear, or symmetric) *function of one variable*. However, for the 12-parameter family of odd-symmetric piecewise-linear vector fields, the topological conjugacy of the unfolded Chua's circuit applies only to the case when the $v_R - vs. - i_R$ characteristic is odd-symmetric with three piecewise-linear segments having an inner slope G_a and an outer slope G_b, such as those depicted below: (b) $G_a < G_b \leq 0$, (c) $G_b < G_a \leq 0$, (d) $G_a \leq 0$, $G_b \geq 0$, (e) $G_b > G_a \geq 0$, (f) $G_a \geq 0$, $G_b \leq 0$, (g) $G_a > G_b \geq 0$.

family of arbitrary odd-symmetric piecewise-linear three-dimensional systems with three regions of linearity (except for a set of zero measure in the parameter space) is mapped into the global unfolding of Chua's circuit in a natural way. A more detailed consideration of this question is presented in Sec. 2 where also a number of typical shapes of attractors taking place at different values of λ and ν are given (see Table 1).

The most thorough analysis devoted to a rigorous proof of the existence of chaos in Chua's circuits was carried out for Eq. (1) [Chua *et al.*, 1986; Silva, 1993] by establishing the existence of homoclinic loops of the saddle-focus at the origin for some values of parameters. Due to symmetry, there exist two homoclinic loops simultaneously, forming a configuration as shown in Fig. 3. After the loops are found, the Shil'nikov theorem is applied which guarantees complicated chaotic behavior of orbits. The bifurcation analysis presented in Chua *et al.* [1986] showed that these loops exist in the region of existence of the double scroll Chua's attractor (Fig. 4) which makes it possible to assert that *the double scroll Chua's attractor is a strange attractor* indeed. Besides, another homoclinic configuration can take place in the region of existence of the double scroll Chua's attractor; namely, a *heteroclinic contour* containing two nontrivial equilibrium states P^+ and P^- of the saddle-focus type and two heteroclinic orbits connecting the equilibria (Fig. 5). These saddle-foci are topologically different from O: $dim\, W^u(P^\pm) = 2$, $dim\, W^s(P^\pm) = 1$. In principle, homoclinic contours of another type (see Fig. 6) studied mathematically by Bykov [Bykov, 1977; 1978; 1980; 1988; 1992] (see also Glendinning & Sparrow [1984] and Bykov & A. Shil'nikov [1989]) are not ruled out in Chua's circuits.

We emphasize that the presence of saddle-focus homoclinic loops implies a number of problems. The crux of the problems is that if the conditions of the Shil'nikov theorem are fulfilled and if the divergence of the vector field is negative at the saddle-focus, then in the bifurcation set of such systems there are dense systems with *infinitely many stable periodic orbits*. This shows that attractors associated with a saddle-focus loop, including the double scroll attractor, cannot be stochastic in a rigorous sense. Furthermore, systems with *nonrough* Poincaré homoclinic orbits (homoclinic tangencies) are also dense in the bifurcation set, which indicates that such attractors are actually *quasiattractors* in the sense of Afraimovich & Shil'nikov [1983]. The problems connected with saddle-focus loops are discussed in Sec. 3, where results obtained by Ovsyannikov and Shil'nikov for the multidimensional case are also presented.

Attractors (quasi) found in Chua's circuits have principal distinctions from, for instance, structurally stable attractors and Lorenz attractors; therefore, there are still many problems of dynamical chaos in Chua's circuits that should be investigated. First, we consider the following question in Sec. 4: if a visible dynamical chaos is observed in a model of this type, what orbit is it associated with? In our opinion, the answer is that such orbits are Poisson-stable orbits whose Poincaré return times are not bounded.

Even the problem of establishing or searching for periodic orbits is not simple. It becomes even more complicated when we have to deal with nonperiodic Poisson-stable orbits. Actually, reasonable

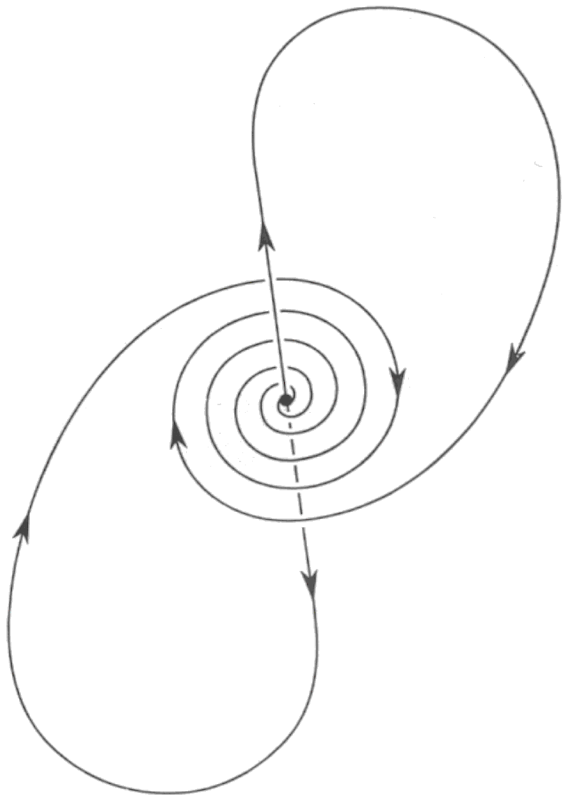

Fig. 3. Two coexisting homoclinic loops originating from a saddle-focus equilibrium point located at the origin of an odd-symmetric vector field.

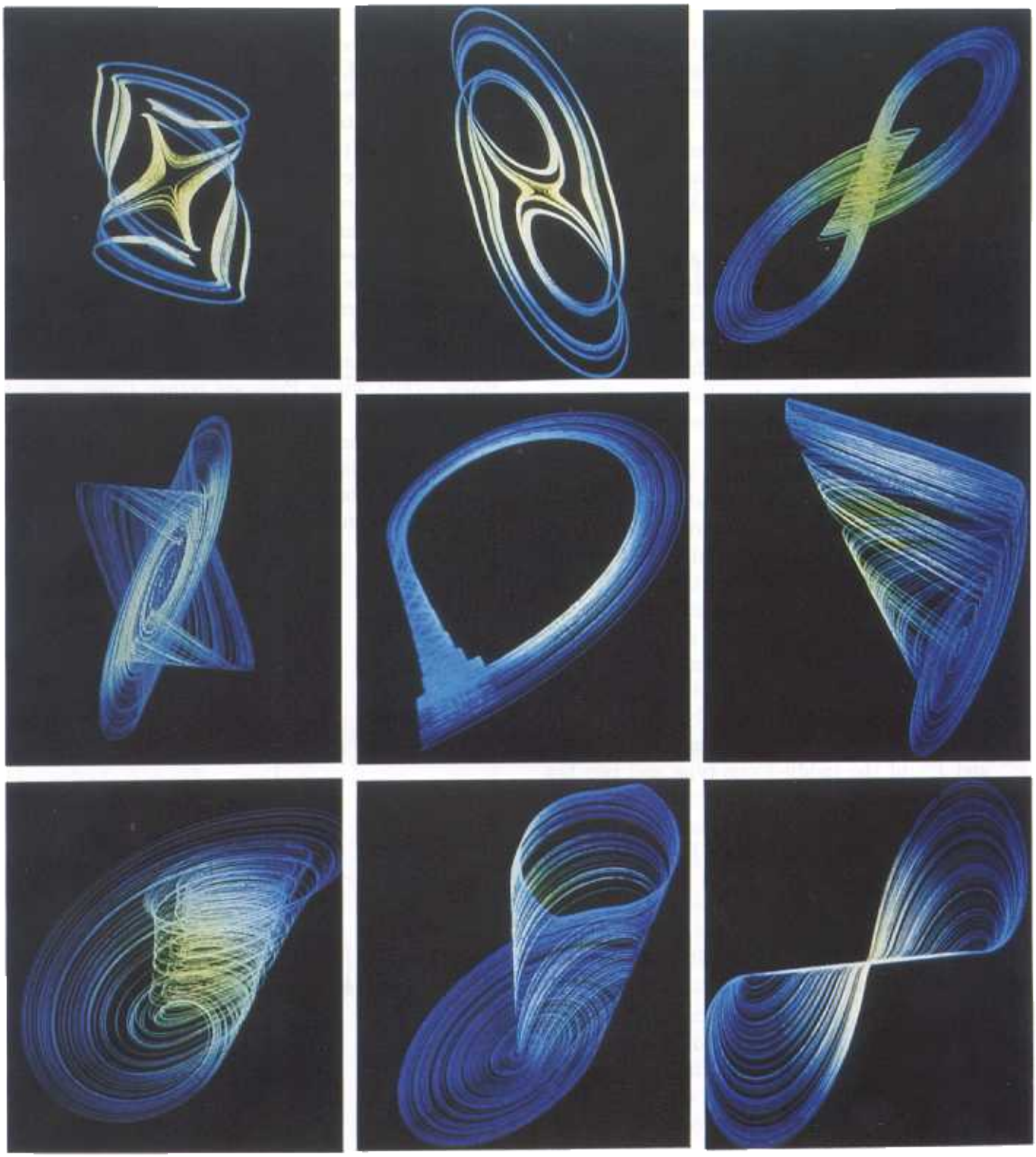

Table 1. A gallery of some strange attractors from the unfolded Chua's circuit

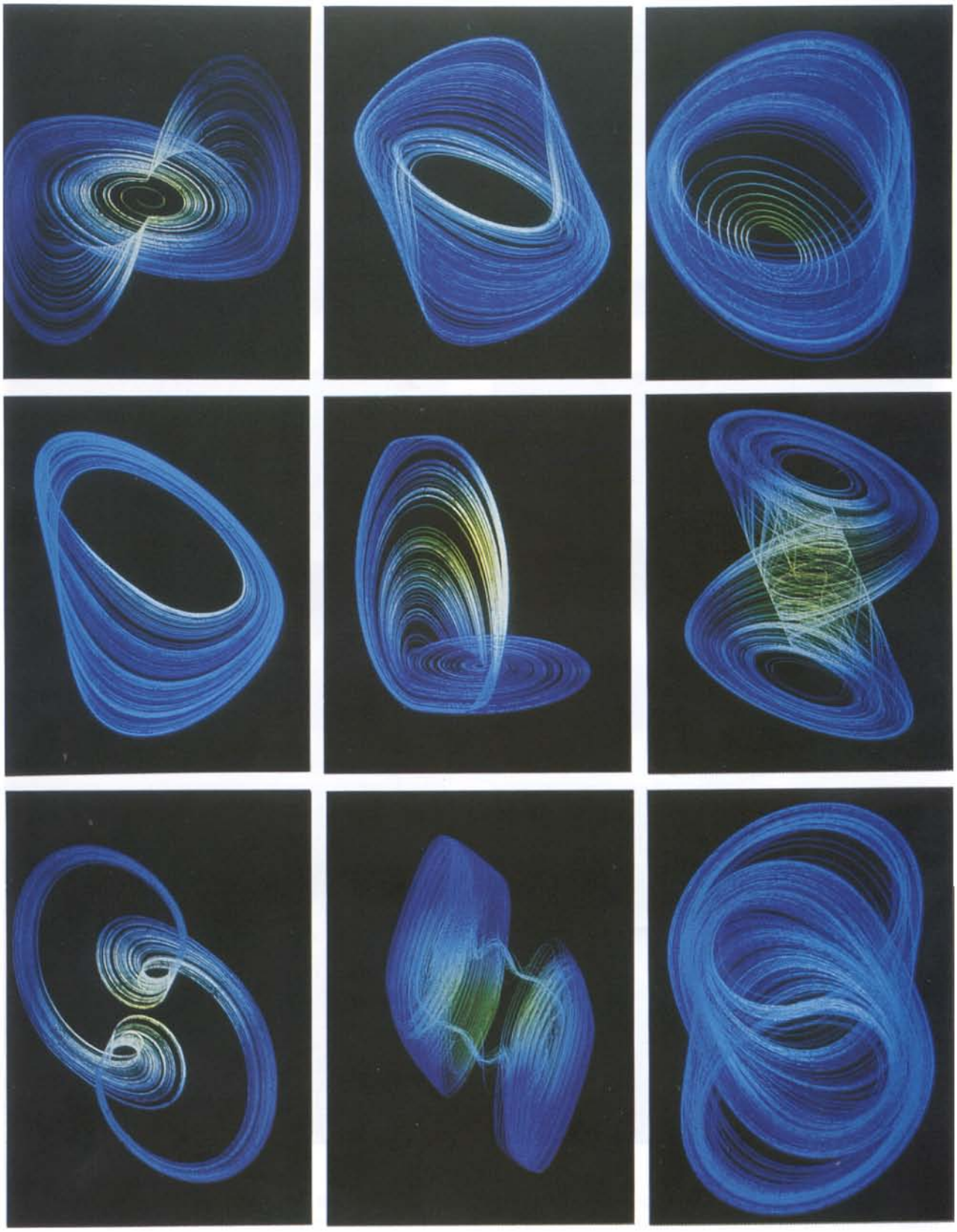

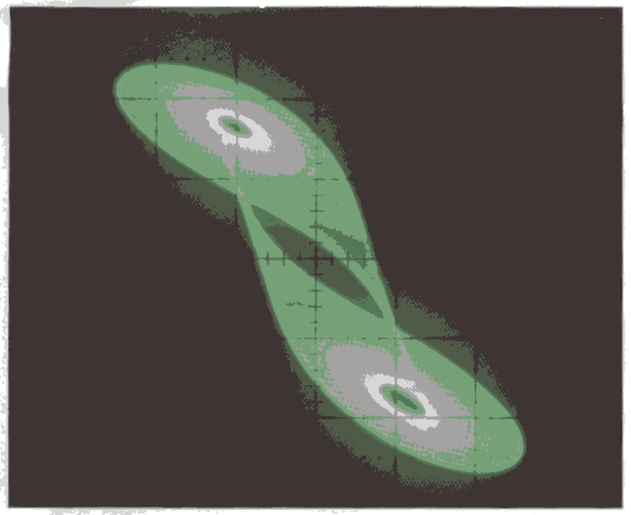

(a.1)

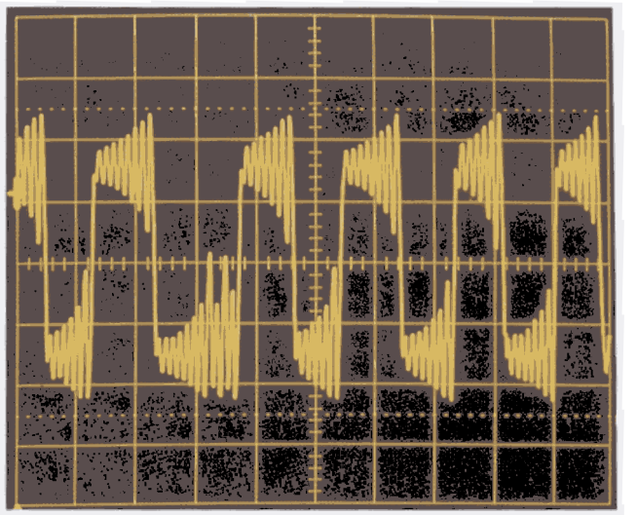

(a.4)

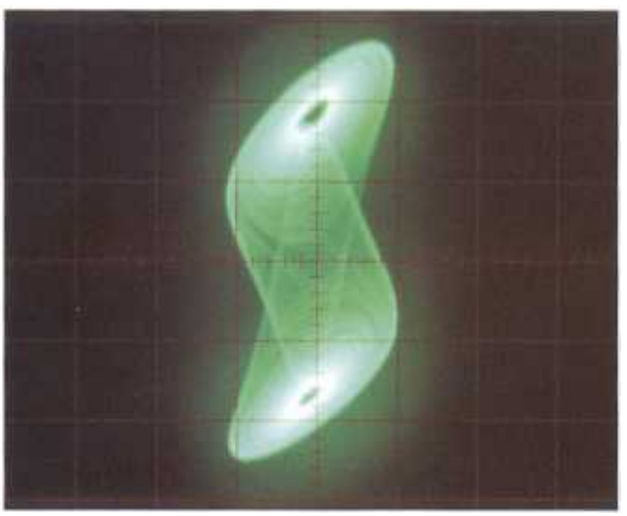

(a.2)

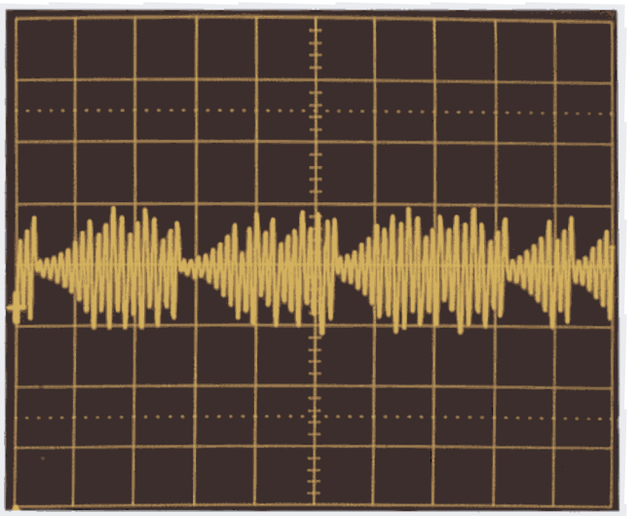

(a.5)

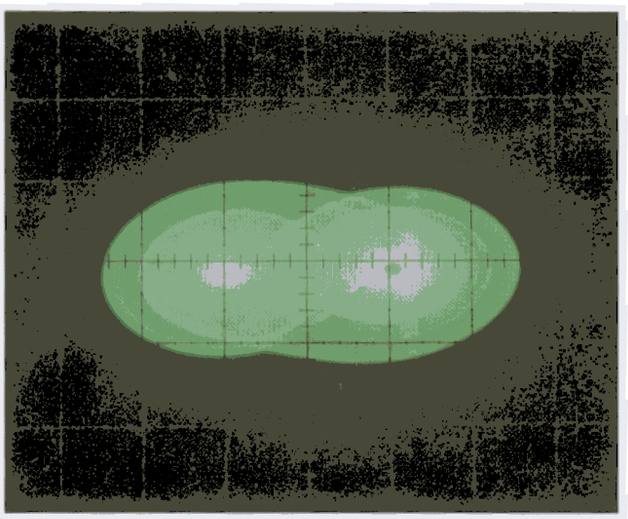

(a.3)

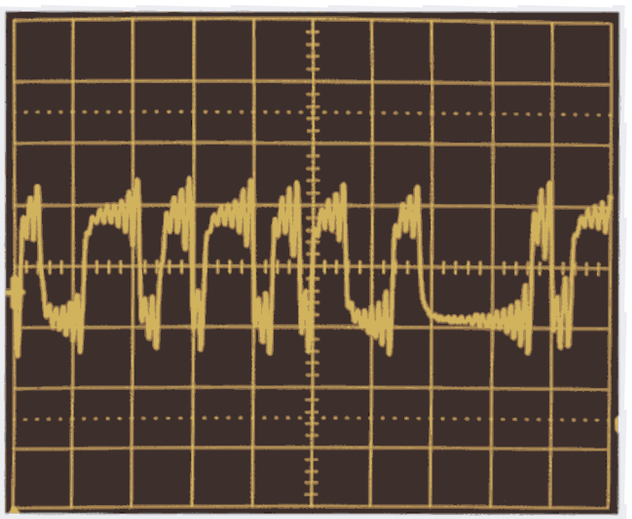

(a.6)

Fig. 4. Experimental and computer-calculated double-scroll Chua's attractor. All experiments are made using the Chua's Circuit IC Chip shown in Fig. 1(d). (a) Projections of the *experimental* chaotic attractor in the v_{C_1}-vs.-i_L plane (a.1), v_{C_1}-vs.-v_{C_2} plane (a.2), v_{C_2}-vs.-i_L plane (a.3), using two of the three time waveforms $v_{C_1}(t)$ in (a.4), $v_{C_2}(t)$ in (a.5), and $i_L(t)$ in (a.6).

Fig. 4. (b) Computer-calculated chaotic attractor from the *dimensionless* Chua's Equation (1) with $\alpha = 15.6$, $\beta = 25.58$, $m_0 = -8/7$, $m_1 = -5/7$.

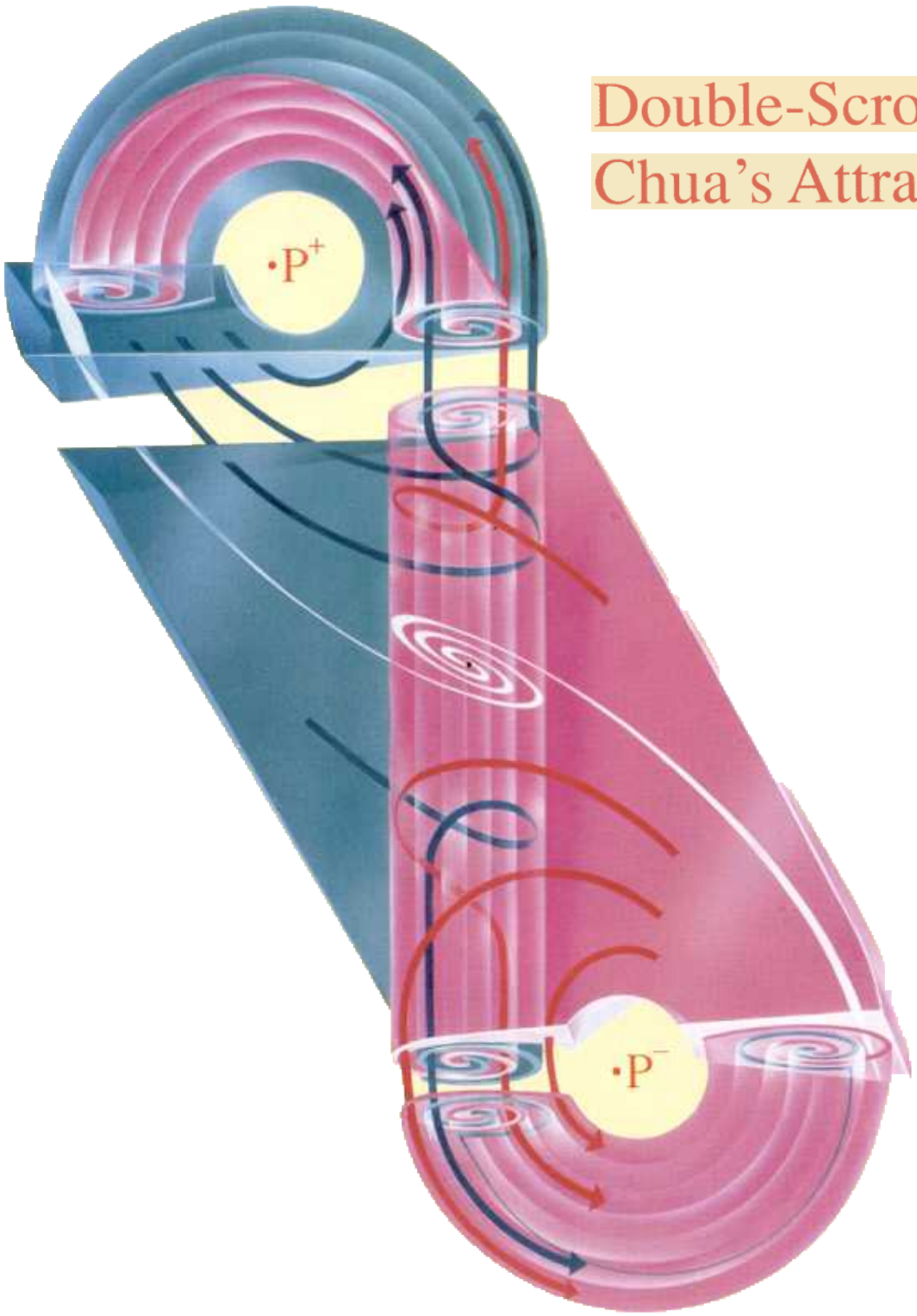

Fig. 4. (c) Schematic illustration of the "macroscopic" structure of the *double-scroll Chua's attractor*. Several typical trajectories are shown in dark blue and in dark red. Two odd-symmetric *homoclinic orbits* at the origin (a saddle-focus) are depicted by a pair of white concentric orbits. Each horizontal cross section (perpendicular to the paper) across the attractor shows, on a macroscopic scale, two concentric spirals. Hence the macroscopic structure of the attractor consists roughly of two concentric scrolls whose ends are gently shaped into two smooth circular caps. On a finer scale, each concentric layer in turn looks like infinitely many infinitesimally thin layers typical of a fractal set. The white hole at the upper (respectively, lower) end cap contains an equilibrium point of the saddle focus type which is generally denoted by P^+ (respectively, P^-) in the literature.

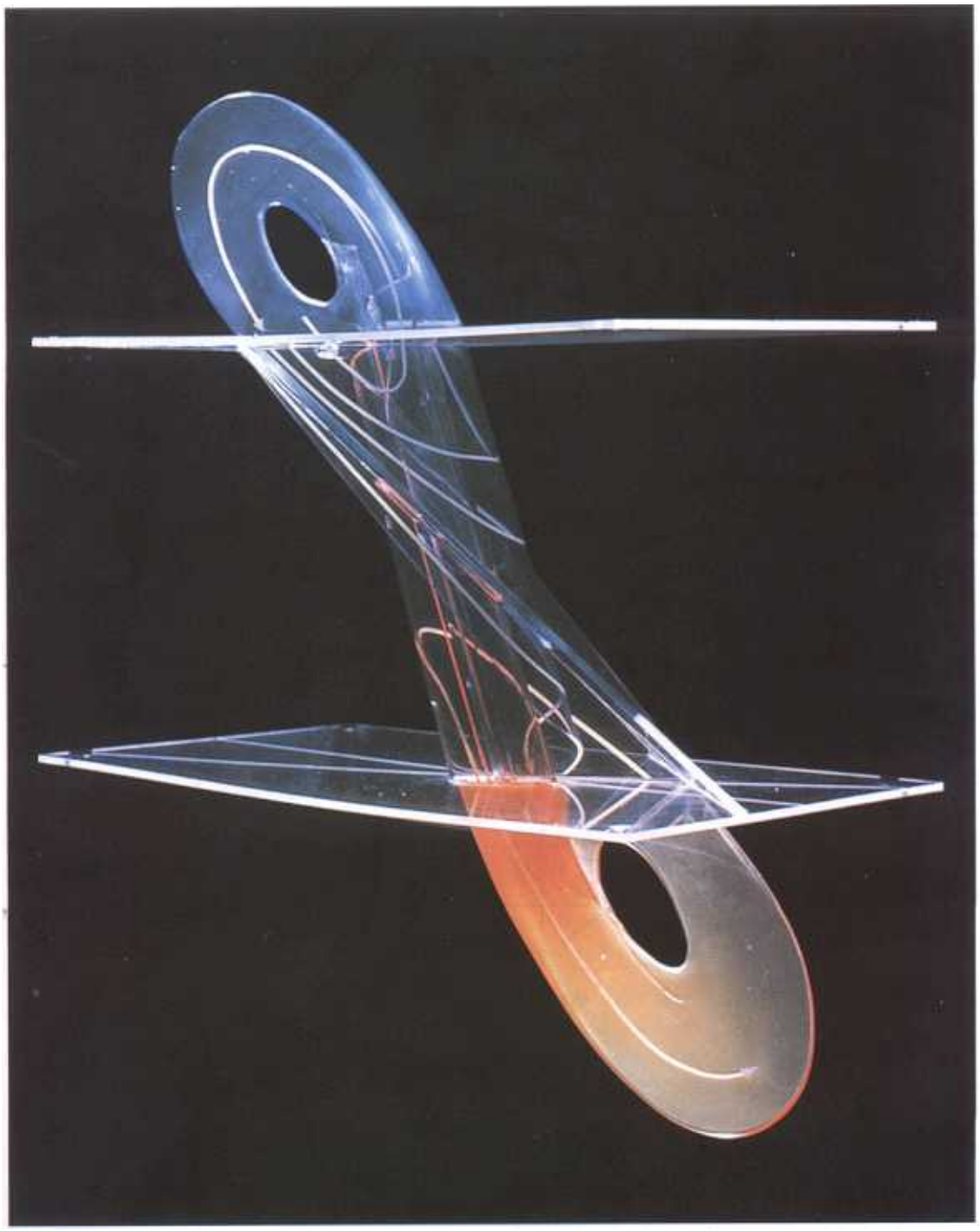

Fig. 4. (d) Three-dimensional fiberglass scaled model of the chaotic attractor calculated and scaled to approximately 20 cm × 80 cm × 100 cm in size from the (x-y-z)-coordinates (x is the vertical axis) of points lying on the attractor. The two horizontal fiberglass planes located at $x = 1$ and $x = -1$ represent respectively the upper and lower boundaries which partition the (x-y-z)-space into three odd-symmetric piecewise-linear regions. The oblique fiberglass plane through the origin (located at the center of the model) is the two-dimensional stable manifold W^s of the saddle-focus equilibrium point at the origin. For certain parameters, two *spiral* Chua's attractors coexist and are separated by this eigenspace in the middle linear region. The double-scroll Chua's attractor is born when these two spiral attractors merged with each other during a codimension-1 bifurcation. Note the thickness of the lower end cap is thickest at the foreground (bright red region) and tapers off to a thin edge at the rear (light red region). In view of the odd symmetry of the vector field, the upper end cap is thickest at the rear (dark blue) and tapers to a thin edge in front (light blue). This three-dimensional model represents the *closure* of the double-scroll Chua's attractor, which is a fractal with a Lyapunov dimension of 2.13 for the parameters used in calculating this model (photograph courtesy of Dr. Ray Brown).

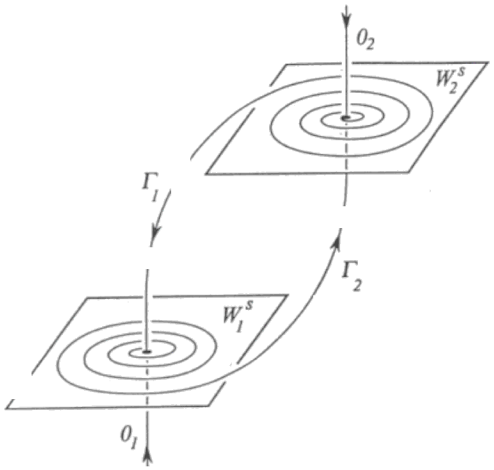

Fig. 5. A homoclinic contour consisting of two saddle foci O_1 and O_2, connected to each other by a pair of heteroclinic orbits Γ_1 and Γ_2. Each saddle focus is characterized by an unstable two-dimensional invariant manifold W^u and a stable one-dimensional manifold W^s.

sufficient conditions for the existence of such orbits are needed. One such criteria is the Shil'nikov theorem. Naturally, this theorem does not resolve all questions, therefore, we give the most universal criterion for dynamical chaos; namely, the presence of a rough (i.e., structurally stable) *Poincaré homoclinic orbit*, i.e., an orbit which is homoclinic to a *periodic orbit*.

Nonwandering sets lying near the homoclinic loop of a saddle-focus, or near a Poincaré homoclinic orbit, are not attractive. To produce dynamical chaos, these sets should be contained in an attractor. In Sec. 5 we give a classification of attractors known to date. Special attention is paid to quasiattractors, which are the most complicated and are very sensitive to variations of parameters. The reason for this is that either the system itself, or a nearby system, possesses a homoclinic tangency within the quasiattractor.

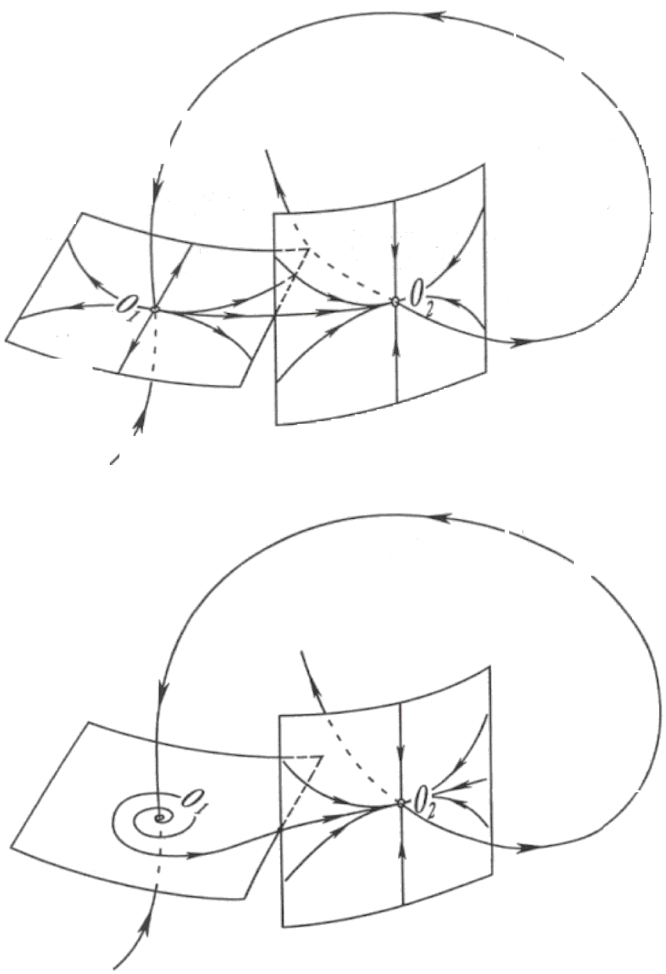

Fig. 6. Two other distinct homoclinic contours which may exist in Chua's circuit.

Problems associated with homoclinic tangencies are discussed in Sec. 6 for both three-dimensional and multidimensional cases. Here, of foremost interest, is the behavior of systems in the so-called Newhouse regions where structurally unstable systems with homoclinic tangencies are dense. In particular, the results presented in this section allows us to predict new phenomena which are possible in Chua's circuits, or coupled Chua's circuits, which are described by equations of dimensions three or higher. We assert, for instance, that in the multidimensional case, together with a "large" attractor there can exist stability windows exhibiting not only periodic and quasiperiodic orbits, but also "small" strange attractors, e.g., attractors similar to the Lorenz attractor and to the double scroll Chua's attractor.

2. Unfolding Chua's Circuit

Systems (1) and (3) above belong to the following class of piecewise-linear systems:

$$\dot{x} = \begin{cases} Ax + b & x_1 \geq 1\,, \quad (4a) \\ Ax - b & x_1 \leq -1\,, \quad (4b) \\ A_0 x & |x_1| \leq 1\,, \quad (4c) \end{cases}$$

where $x = (x_1, x_2, x_3)$, $A = (a_{ij})_{i,j=1,2,3}$, $b = (b_1, b_2, b_3)^T$, $A_0 = (\alpha_{ij})_{i,j=1,2,3}$.

By imposing the condition of continuity of the right-hand sides, it is easy to show that Eq. (4) can be recast into the following equivalent but more compact form

$$\dot{x} = Ax + \frac{1}{2}\{|\langle w, x\rangle + 1| - |\langle w, x\rangle - 1|\}b\,, \qquad (5)$$

where A and b are as defined above, $w = (1, 0, 0)^T$, and $\langle \cdot, \cdot \rangle$ denotes the vector dot product. Observe that for $x_1 \geq 1$, Eq. (5) reduces to Eq. (4a), and for $x_1 \leq -1$, Eq. (5) reduces to Eq. (4b). Similarly, when $|x_1| \leq 1$, Eq. (5) reduces to Eq. (4c), upon identifying

$$A_0 = A + \begin{bmatrix} b_1 & 0 & 0 \\ b_2 & 0 & 0 \\ b_3 & 0 & 0 \end{bmatrix}.$$

The continuous family (5) has twelve independent parameters. Let us denote it by E^{12}. The following theorem is valid [Chua, 1993]:

Theorem 1. *Let λ and ν be the sets of eigenvalues of matrices A_0 and A respectively for a system belonging to $E^{12}\backslash E_0$ where E_0 is a set of zero measure in the parameter space of Eq. (5). Then, the system is linearly equivalent to the unfolded Chua's circuit (3) with the same sets λ and ν.*

In other words, the unfolding of Chua's circuit is a canonical representative of, practically, the entire twelve-parameter family of piecewise-linear odd-symmetric systems with three domains of linearity. We must emphasize here that the above assertion is concerned only with linear equivalence and piecewise-linear systems. This is because if we consider the smooth analogues of Chua's circuits, it would be senseless to try to find a canonical representative for such systems with respect to topological equivalence. The reason is that a complete description of systems in the Newhouse regions (see Sec. 6) requires infinitely many invariants [Gonchenko *et al.*, 1992; 1993a; 1993c], but these regions are actually present in the parameter space of Chua's circuits, for instance, near the parameter values corresponding to saddle-focus homoclinic loops (Sec. 3).

The theorem above shows that (λ, ν) are the natural control parameters for the unfolded Chua's circuit. That is why we display their values in Fig. 7 together with the values of the associated physical parameters (a rather simple connection between physical parameters and the sets of eigenvalues is given in Chua [1993]).

An examination of the strange attractors shown in Figs. 7(a)–7(i) reveals the following two properties:

1. The eigenvalues $\lambda = (\lambda_1, \lambda_2, \lambda_3)$ associated with the attractors shown in Figs. 7(a)–7(i) can be real or complex numbers. We will see in the next section that this is not accidental. The equilibrium state O may be either a saddle, or a saddle focus, and either one can be totally unstable.
2. Strange attractors exist in both cases when the vector field has a negative divergence [Fig. 7(b)], and when the divergence in the inner and in the outer regions have opposite signs [the sign of divergence is determined by $(\lambda_1 + \lambda_2 + \lambda_3)$ for $|x| \leq 1$, and by $(\nu_1 + \nu_2 + \nu_3)$ for $|x| \geq 1$]. This is important because in three-dimensional systems having divergence of nonconstant signs, structurally stable periodic orbits of all three possible topological types can coexist in an attractor. Also, variations in the signs of the divergence is necessary in order for a transition to chaos to occur through the breakdown of an invariant torus.

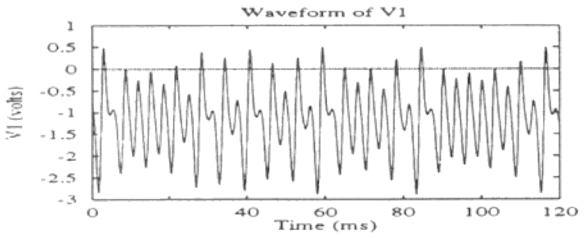

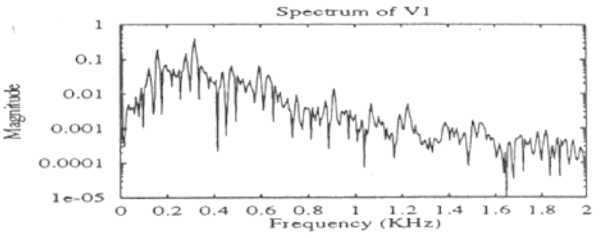

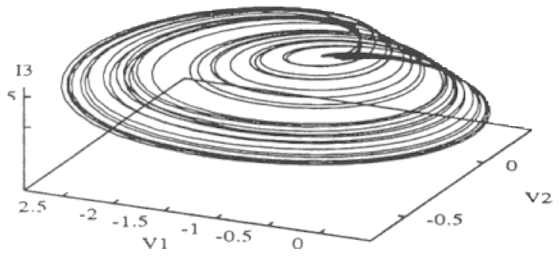

(a) $C_1 = -149nF$, $C_2 = 1\mu F$, $L = -658mH$, $G_a = -1.14mS$, $G_b = -0.714mS$, $R = 1K\Omega$.
Eigenvalues: $\lambda_1 = 16.4$, $\lambda_2 = -1.08\times10^3+2.33\times10^3 i$, $\lambda_3 = -1.08\times10^3 - 2.33\times10^3 i$, $\nu_1 = -672$, $\nu_2 = 796 + 1.93\times10^3 i$, $\nu_3 = 796 - 1.93\times10^3 i$.

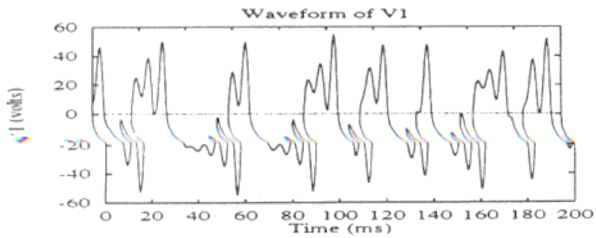

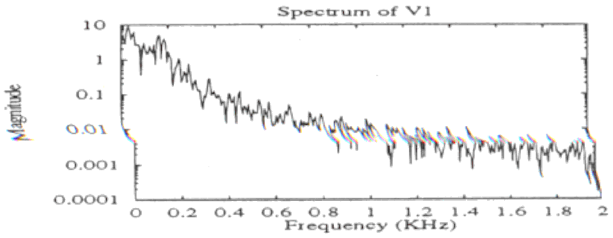

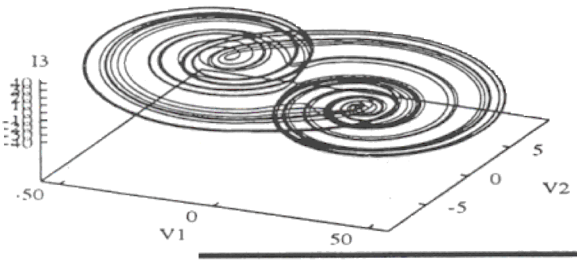

(b) $C_1 = -203nF$, $C_2 = 1\mu F$, $L = -274mH$, $G_a = -2.497mS$, $G_b = -0.9301mS$, $R = 1K\Omega$.
Eigenvalues: $\lambda_1 = -6.34\times10^3$, $\lambda_2 = -3.31\times10^3$, $\lambda_3 = 1.28\times10^3$, $\nu_1 = -992$, $\nu_2 = 168+1.11\times10^3 i$, $\nu_3 = 168 - 1.11\times10^3 i$.

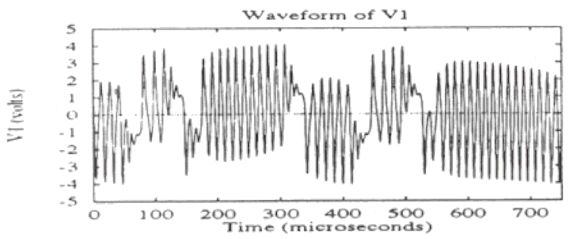

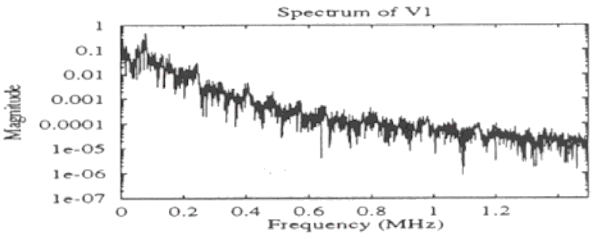

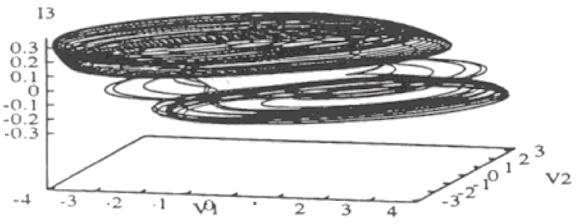

(c) $C_1 = -768.6pF$, $C_2 = 1nF$, $L = -73.5mH$, $R = 1K\Omega$, $R_0 = 2.18K\Omega$, $G_a = 0.169mS$, $G_b = -0.477mS$.
Eigenvalues: $\lambda_1 = 7.84\times10^5$, $\lambda_2 = -3.37\times10^5$, $\lambda_3 = 1.03\times10^5$, $\nu_1 = 1.52\times10^4$, $\nu_2 = -1.53\times10^5 + 7.61\times10^5 i$, $\nu_3 = -1.53\times10^5 - 7.61\times10^5 i$.

Fig. 7. Some strange attractors observed from the unfolded Chua's circuit. Each attractor is shown in the three-dimensional space (V_1, V_2, I_3), which is equivalent to the (x, y, z)-space of the *dimensionless* unfolded Chua's equation. Also shown is a segment of the time waveform $V_1(t)$ and its power spectrum. The values of the associated circuit parameters are also given, along with the eigenvalues $(\lambda_1, \lambda_2, \lambda_3)$ at the equilibrium point at the origin, and the eigenvalues (ν_1, ν_2, ν_3) at the equilibrium points P^+ and P^- (located in the outer affine region), which are identical due to symmetry.

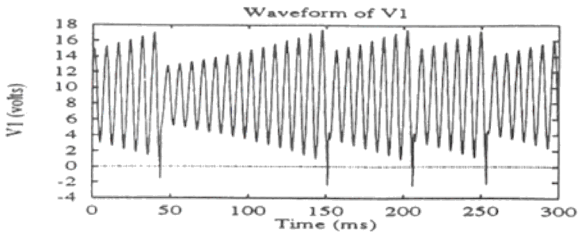

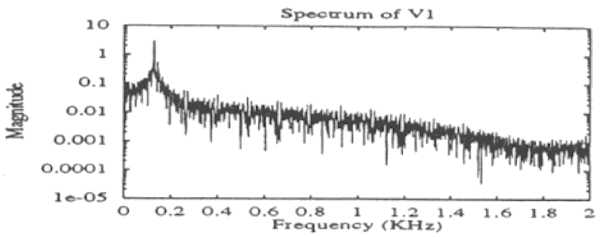

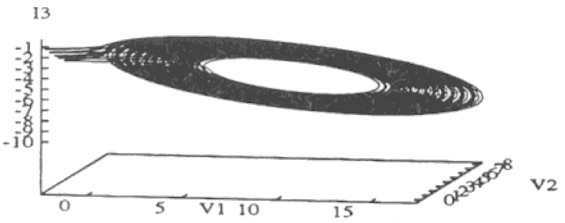

(d) $C_1 = 57.5nF$, $C_2 = -1\mu F$, $L = -708mH$, $R = 1K\Omega$, $R_0 = 740\Omega$, $G_a = -1.525mS$, $G_b = -0.458mS$.
Eigenvalues: $\lambda_1 = 5.56 \times 10^3$, $\lambda_2 = 3.61 \times 10^3$, $\lambda_3 = 1.57 \times 10^3$, $\nu_1 = -7.40 \times 10^3$, $\nu_2 = -18.2 + 854i$, $\nu_3 = -18.2 - 854i$.

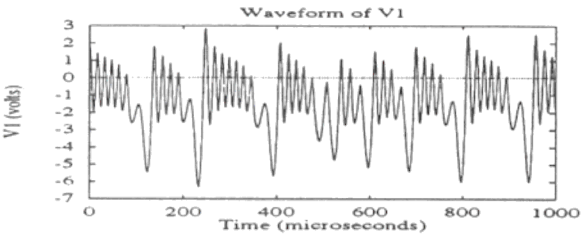

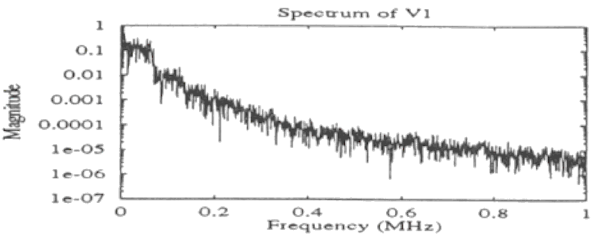

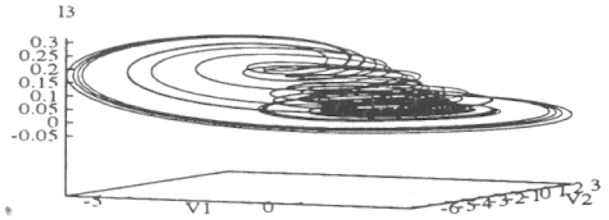

(e) $C_1 = 811pF$, $C_2 = -1nF$, $L = -138mH$, $R = 1K\Omega$, $R_0 = 12.1K\Omega$, $G_a = -0.177mS$, $G_b = -0.02mS$.
Eigenvalues: $\lambda_1 = 5.28 \times 10^4$, $\lambda_2 = 1.00 \times 10^4 + 4.72 \times 10^5 i$, $\lambda_3 = 1.00 \times 10^4 - 4.72 \times 10^5 i$, $\nu_1 = -2.08 \times 10^5$, $\nu_2 = 4.35 \times 10^4 + 1.73 \times 10^5 i$, $\nu_3 = 4.35 \times 10^4 - 1.73 \times 10^5 i$.

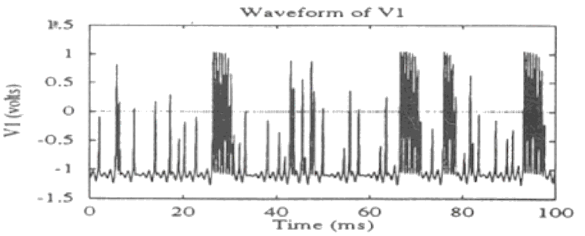

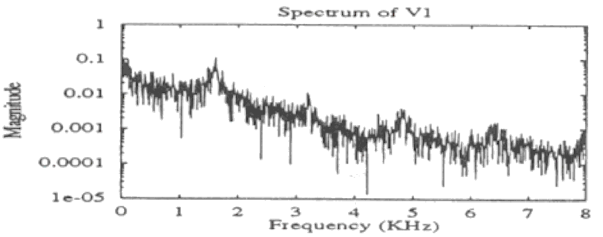

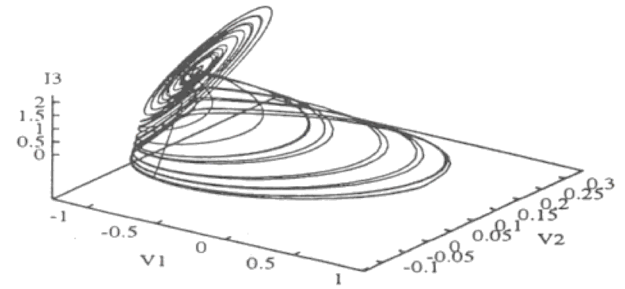

(f) $C_1 = -13.33nF$, $C_2 = 1\mu F$, $L = 32mH$, $R = 1K\Omega$, $R_0 = -100\Omega$, $G_a = -0.98mS$, $G_b = -2.4mS$.
Eigenvalues: $\lambda_1 = 2.67 \times 10^3$, $\lambda_2 = 480 + 1.02 \times 10^4 i$, $\lambda_3 = 480 - 1.02 \times 10^4 i$, $\nu_1 = -1.04 \times 10^5$, $\nu_2 = 700 + 5.06 \times 10^3 i$, $\nu_3 = 700 - 5.06 \times 10^3 i$.

Fig. 7. (*Continued*)